

Effects of Synthesis Conditions on Magnetic Field Sensitive Colloidal Nanoparticle Properties

Serhat Küçükdermenci ^{*,1}

¹Department of Electrical and Electronics Engineering, Faculty of Engineering, Balıkesir University, 10463, Balıkesir, Turkey.

*corresponding author email: kucukdermenci@balikesir.edu.tr

Abstract – The first step for new developments in nanotechnology, which includes the design, fabrication and functional use of nanostructured materials and devices, is the synthesis of nanoparticles. The size of nanoparticles in magnetic fluids can be controlled by various synthesis methods. In addition to particle size, the use of surfactants can also add new features to the system. Particles that are generally well soluble in water are easy to use for some applications. Magnetic fluids, in other words ferrofluids, are colloidal suspensions of magnetic nanoparticles. Magnetic fluids are a hybrid structure with fluidity of fluid and magnetism of solid magnetic materials. These structures, which react to the magnetic field, can be used in magneto-optical and magneto-caloric studies. In this study, "high temperature hydrolysis reaction" method was used to synthesize magnetic field sensitive colloidal nanoparticles. In order to observe the effects of the change in reaction conditions on the synthesis, the main synthesis conditions to be compared later were determined. Modified syntheses were formed by changing one of the main synthesis reaction conditions and keeping the others constant, and the effects of the changed condition on the synthesis were observed. In the study, the effects of NaOH/DEG ratio, PAA amount, FeCl₃ amount and reaction temperature criteria on the synthesized particle were investigated. Thus, an idea has been gained about how these properties should be adapted to synthesize particles with the desired properties.

Keywords – Nanoparticles, Water-Soluble, Poly(Acrylic Acid), Magnetic Fluids, Colloidal Nanoclusters, High Temperature Hydrolysis;

I. INTRODUCTION

Nanoparticle production methods are chemical vapor deposition [1], hydrogen reduction method [2], inert gas condensation method [3], micro heterogeneous system [4], flame spray pyrolysis [5] and co-precipitation [6] and high temperature hydrolysis reaction method [7]. Among them, the high temperature hydrolysis reaction method is performed using the "Schlenk line" as it requires an airless environment [8].

Recently, studies on the development of high quality nanoparticles whose size and shape can be controlled by various synthesis methods have accelerated [9]. Researches on the tendency of nanoparticles to form secondary structures both

"self-assembly" and directly through solution growth, continue in the last years [10].

Colloidal nanoclusters (CNC) show superparamagnetic properties at room temperature, whereas single-crystal magnetite particles want to exhibit ferromagnetic behavior in the same size range. High magnetization and good water-soluble superparamagnetic behavior make CNCs the ideal material for many important applications such as drug delivery, biodegradation, and magnetic resonance imaging.

Superparamagnetic nanoparticles appear to be very promising in biomedical applications [11]. Iron oxide nanoparticles have become a very attractive material due to their stability and biocompatibility under physiological conditions. Many applications

have been developed by synthesizing magnetic iron oxide nanoparticles in non-polar solvents, at increasing temperatures, in organometallic processes, by controlling the size distribution [12]. For biomedical applications, the transfer of hydrophobic nanoparticles from non-polar solvent to water is also often implemented with the addition of surface modification [13]. Since each of the nanoparticles prepared by this method, about 10 nm in size, has low magnetization, it is difficult to effectively separate them from the solution. Therefore, the use of these materials in some practical applications is limited. Increasing the nanoparticle size increases the saturated magnetization and creates a superparamagnetic-ferromagnetic transition, so the solubility of these nanoparticles in solution is not long-lived. While the magnetite nanoparticle clusters are synthesized, the desired behavior of the particle is to maintain its superparamagnetic properties and to increase the magnetization in a controlled manner [14].

Very well water-soluble magnetite CNCs can be produced by high temperature hydrolysis method using polyacrylic acid (PAA) [15] as a surfactant. Iron(III) chloride is used as the precursor in the synthesis and diethylene glycol is the polar solvent. The reason for using PAA in production is to provide strong coordination of carboxylate groups with iron cations on the magnetite surface. When the mixture of NaOH (sodium hydroxide) and DEG (Diethylene Glycol) (stock A) is transferred to the other mixture (stock B) consisting of FeCl₃ and PAA, the alkalinity of the reaction increases and it occurs with the hydrolysis of FeCl₃. In a reducing atmosphere (nitrogen environment) at high temperatures, Fe(OH)₃ is partially converted to Fe(OH)₂ with the help of DEG, and finally, Fe₃O₄ is formed with the dehydration of its particles. Under optimized conditions, Fe₃O₄ nanoparticles spontaneously assemble into three-dimensional clusters.

It is seen from previous studies that the size distribution of CNCs can be fully controlled between 30–180 nm by simply increasing the amount of NaOH provided all other parameters remain the same. High H₂O concentration and strong alkalinity can increase the hydrolysis of FeCl₃ and form extensive oxide formation. The growth of CNCs is explained by the two-step growth model method, in which primary nanoparticles are first aggregated in the form of supersaturated

solution and then large secondary particles [16]. CNCs exhibit superparamagnetic behavior at room temperature, the external magnetic field response is stronger than magnetite nanoparticles due to the magnetization of each particle [17].

A. Magnetic fluids

Magnetic fluids are colloidal structures in which magnetic particles ranging in size from 1 to 500 nm are dispersed in a carrier fluid, having both the magnetic properties of solids and the fluidity properties of liquids. Components that make up the magnetic fluid; magnetic particles are shown in Figure 1 as liquid carrier and surfactant. Since their synthesis in the 1960s, the applications of magnetic fluids in technological fields have increased steadily [18]. Although magnetic fluids are isotropic Faraday rotation, birefringence, etc., by showing anisotropic properties with the applied external magnetic field exhibit magneto-optical effects. Magnetic particles should be coated with a suitable material to prevent aggregation of magnetic particles. According to this coating process, magnetic fluids are divided into two groups as superficial and ionic.

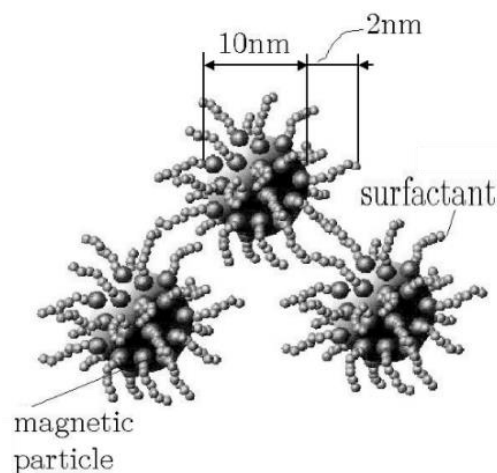


Fig. 1 Diagram of magnetic fluid particles with surfactant (for clarity, particles and surfactant molecules are not depicted in scale).

A. Surfacted magnetic fluid

Chemical surfactant molecules are used for coating. By forming an energy barrier by the surface agent molecules, the attractive forces that occur in neutral atoms and molecules are prevented and stability is ensured. Particles can be dispersed in a polar or non-polar liquid. If the particle is dispersed in a non-polar liquid (e.g., oil), a single layer of surface agent is needed to form an external

"hydrophobic" layer. The polar head of the surfactant is attached to the surface of the particle and now has a carbonic chain structure between it and the carrier liquid. On the other hand, when the particle is dispersed in a polar medium (e. g. water), a double layer of chemical surface agent is needed to form a "hydrophilic" layer. The polar head of the surfactant may be "cationic," "anionic," or non-ionic. In Figure 2(a), oil-based representation is drawn and in Figure 2(b), water-based representation is drawn.

B. Ionic magnetic fluid

The coating is an electrically charged shell. To maintain the stability of the colloidal system, the nanoparticles in the ionic magnetic fluid are electrically charged. In the magnetic particle precipitation method, using acid or alkaline reaction, their surfaces are obtained as electrically charged. Water is generally used as the carrier liquid and the pH value of the solution varies between 2-12 according to the surface charge sign of the particle. Acidic excited magnetic fluid with pH less than 7 has positively charged particles, while basic excited magnetic fluid with pH value greater than 7 has negatively charged particles. The surface charge density is typically around $10 \mu\text{C}/\text{cm}^2$. In Figure 2(c) and 2(d), acidic and basic notations are given as examples of ionic magnetic fluid.

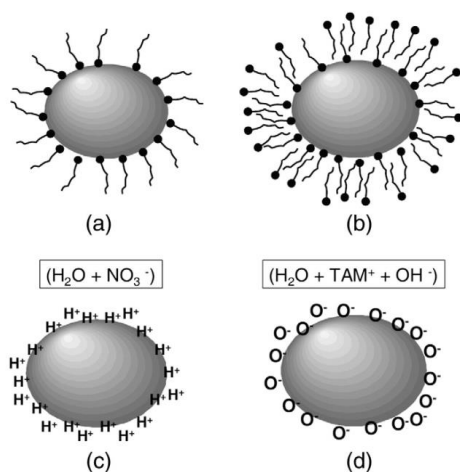


Fig. 2 Coated magnetic particles (a) single layer and (b) double layer Ionic magnetic fluid (c) acid magnetic fluid grain and (d) alkaline magnetic fluid grain (here TAM+OH- is the tetramethylammonium hydroxide).

In this study, the high temperature hydrolysis reaction, one of the ferrofluid synthesis methods, is described in detail, taking into account the variable synthesis conditions. The synthesis of "mono"

(singular) dispersed magnetite colloidal clusters by high temperature solution phase process is emphasized. In the studies, it was seen that the size of the clusters could be regulated by changing the hydrolysis rate with the effect of NaOH. PAA chains attached to the surface form highly water soluble aggregates.

II. MATERIALS AND METHOD

Chemicals used in synthesis are diethylene glycol (DEG, 99.9%), ferric chloride (FeCl_3 , 97%), sodium hydroxide (NaOH, 96%), and polyacrylic acid (PAA, Mw = 1,800) from Sigma-Aldrich. Distilled water was used in all syntheses. All chemicals were used without further processing and/or purification. The flow chart for the high temperature hydrolysis method used for the synthesis is shown in Figure 3.

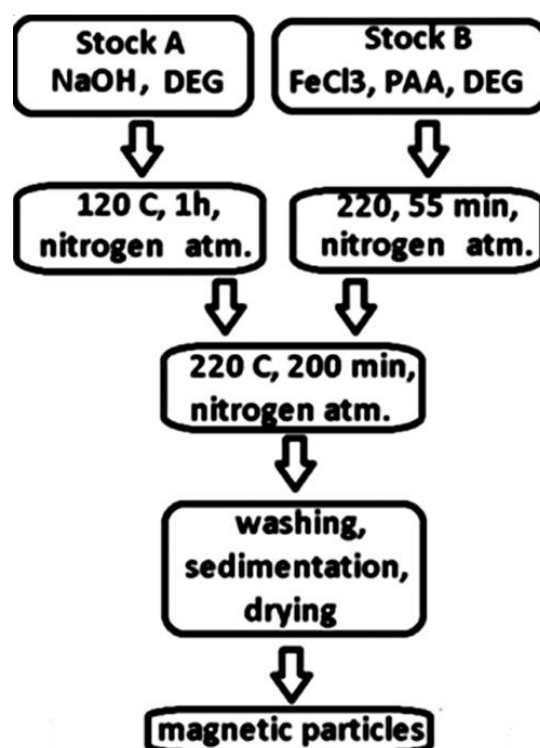


Fig. 3 Flow chart of the synthesis.

The NaOH/DEG solution was obtained by heat treatment of 100 mmol NaOH with 40 mL DEG at 120 °C for 1 hour in nitrogen environment. This stock solution (Stock A) was kept at 70 °C to be injected into the second solution to be prepared. The second solution (Stock B) was prepared by dissolving 10 mmol FeCl_3 and 20 mmol PAA in 41 mL DEG in a 100-mL nitrogen inlet and reflux-mounted three-neck flask and heat treatment at 220 °C for 50 minutes. 20 mL of stock A solution

was rapidly injected into stock B, and the heat treatment was continued for another 2 hours. After the reaction, the particles were washed with ethanol and water, collected with the help of a magnet and dried.

The “Schlenk line” is a system used in the production of nanoparticles (Figure 4). In this system, there is a double-way tapped manifold in the centre to prevent moisture and oxygen from entering the atmosphere. Thus, when the tap is turned in one direction, when the nitrogen inlet is turned to the other side, a connection to the vacuum is ensured.

The “bubble counter” at the end of the nitrogen line prevents air from entering the system and also indicates the nitrogen flow in the system. If vacuum is drawn from the bubble counter, there is a risk of both air and bubble counter fluid entering the system. In such a case, the line will have to be cleaned again. If it is necessary to remove the vacuum above the nitrogen line, the clamp on the top of the hose must be tightened to prevent it from being reabsorbed from the bubble counter. While the line is in use, nitrogen output from the nitrogen manifold should be steady and slow.

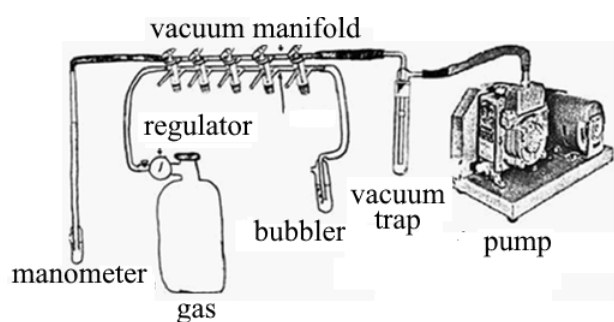


Fig. 4 Schematic representation of the synthesis assembly.

The arrangement of the equipment is important in preventing the solutions from coming into contact with air. The “Schlenk balloon” is a round bottom balloon with a tap inlet. The reason why the hose connected to the manifold is thick is to prevent it from shrinking under vacuum. Schlenk splice funnel or Schlenk filter can be placed on the neck side of the Schlenk balloon. The Schlenk funnel is a convenient tool for adding the solution to the Schlenk flask. By closing the tap slowly, the air comes out from under the balloon and moves away from the line, so the solutions are placed in the funnel without being contaminated with the atmosphere and sent to the balloon. A nitrogen manifold is first connected to the tap inlet to move

the solution from the funnel to the flask. Then only the valve at the bottom of the funnel opens. This is critical for balancing the upper and lower balloon pressure.

Common use is the closure of the Schlenk balloon with a “septum”. The septum is an airtight hose diaphragm. Even if the septum is punctured with various cutting tools, fluid can be added or removed from the balloon without contact with air.

A “syringe” is one of the ways to transfer a liquid into or out of a septum-sealed container. If the container is under nitrogen pressure, the syringe can simply be inserted into the container. Some liquid is withdrawn and the syringe is placed in the other balloon and the liquid is injected. While injecting from one balloon to the other, there should be no air inlet through the injector hole. There are two important tips in using syringes. The first is the removal of air in the injector before transferring fluid. This process is carried out by filling and discharging nitrogen gas into the injector. This process is repeated 2-3 times to clear the air in the syringe. Second, pressure should always be considered in syringe transfer. If an attempt is made to draw liquid from a closed container, this cannot be done without increasing the partial vacuum in the container.

The “cannula” is a long needle of hollow steel with two sharp ends. Another way of fluid transfer is cannula fluid transfer. If the pressure in one balloon is greater than the other, the liquid will be transferred from the high-pressure balloon to the other.

DTA-TG (Differential thermal analysis - Thermogravimetric) analysis, FTIR (Fourier transform infrared spectroscopy) analysis, XRD (X-ray diffraction) analysis, VSM (Vibrating sample magnetometry) analysis, SEM (Scanning electron microscope) analysis, DLS (Dynamic light) More detailed information on scattering analysis, TEM (Transmission electron microscopy) analysis, synthesis, magneto-optics, magneto-caloric applications can be found in doctoral thesis of Küçükdermenci [19] and his studies [20], [21].

NaOH/DEG ratio, amount of PAA, amount of FeCl₃ and reaction temperature were considered as parameters in modified syntheses while examining the effects of changes in synthesis conditions on particle properties [12].

III. RESULTS

In order to examine the effects of the reaction conditions in the high temperature hydrolysis reaction, first of all, the main synthesis conditions, which will be based on the comparison with the modified syntheses, were studied. The main synthesis conditions can be listed as follows; NaOH is 125 mmol, NaOH/DEG is 2.5 mol/L, DEG is 50 mL, FeCl₃ is 20 mmol, PAA is 40 mmol, stock solution transfer is 40 mL, mixing temperature is 190 °C, heating process is 120 minutes.

Modified syntheses were formed by changing one condition at a time in the main synthesis and keeping the other values constant. Accordingly, the factors that will affect the particle size under the reaction conditions were determined as stock solution A, B and mixture parameters. The NaOH/DEG ratio of stock A, the amount of FeCl₃ and PAA of stock B and the reaction temperature of the mixture are customized experimental parameters.

The main and modified synthesis conditions are given in Table 1. Totally nine synthesis types were revealed. The particles synthesized after washing and drying are shown in Figure 5 collectively.



Fig. 5 General view of the synthesized particles.

Table 1. Main and modified synthesis conditions.

Modification	Description	Code
Main Synthesis	2.5 mol/l	A0
NaOH/DEG Ratio	2 mol/l	B1
	3 mol/l	B2
PAA Amount	0 mmol	D1
	30 mmol	D2
	36 mmol	D3
	50 mmol	D5
FeCl ₃ Amount	15 mmol	E1
	25 mmol	E2
Reaction Temperature	140 Degrees	F1

C. Main synthesis features

For phase structure and size information of magnetic particles the crystal structure of the prepared sample was confirmed by XRD analysis (see Figure 6). (220), (311), (400), (422), (511), and (440) diffraction peaks (JCPDS chart: 19-0629) are in good agreement with the Fe₃O₄ phase.

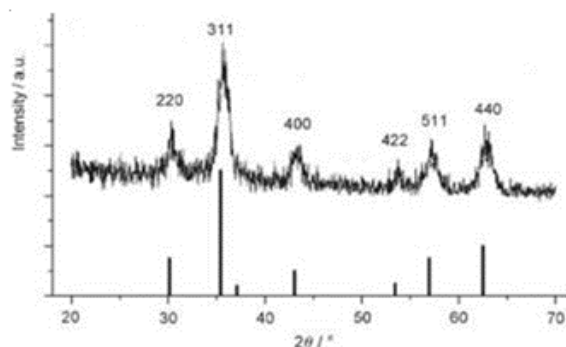


Fig. 6 X-ray powder diffraction pattern (for A0 coded synthesis). (“Bulk” Fe₃O₄ samples, peak positions and relative “intensities” recorded in the literature are shown with vertical bars.)

The average diameter obtained from DLS for the main synthesis is about 10 nm (see Figure 7). The mean diameter calculated by TEM measurement is 8.16 nm (see Figure 8). In the next steps, the effects of parameters such as NaOH/DEG ratio, FeCl₃ amount, PAA amount, reaction temperature on the synthesis were observed.

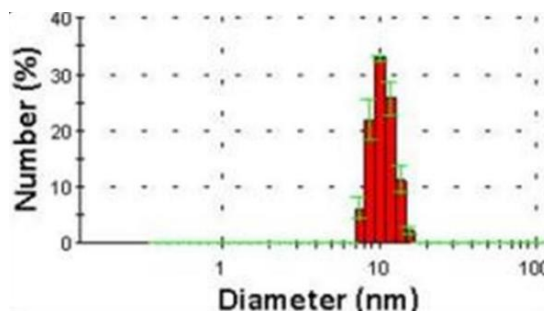


Fig. 7 DLS for A0 coded synthesis.

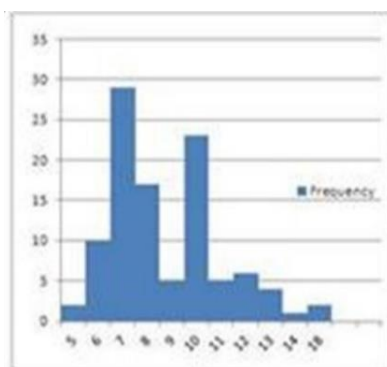


Fig. 8 Average size distribution obtained from TEM for A0 coded synthesis.

D. Effects of NaOH/DEG ratio on synthesis

The experiment of the effects of the NaOH/DEG ratio on the synthesis was arranged according to Table 2. While the particle diameter was found to be approximately 10 nm in the synthesis for 2.5 mol/L transfer, the particle diameter was found to be approximately 2 nm in the 2 mol/L synthesis and around 300 nm in the 3 mol/L synthesis (see Figure 9 and Figure 10).

Table 2. Synthesis conditions determined for the NaOH/DEG effect.

Modification	Description	Code
Main Synthesis	2.5 mol/l	A0
NaOH/DEG Ratio	2 mol/l	B1
	3 mol/l	B2

NaOH in the reaction produces water molecules and increases the alkalinity of the solution by giving hydroxylate anions. It increases the hydrolysis of FeCl₃ in magnetite and forms clumps of increasing size. Adding NaOH to the hot mixture of DEG, FeCl₃ and PAA generates water molecules and also increases the alkalinity of the reaction system, both of which result in FeCl₃ hydrolysis.

This adjustability in length may be due to slight differences in H₂O concentration and the addition of varying amounts of NaOH. High H₂O concentration and stronger alkalinity can accelerate FeCl₃ hydrolysis and support the formation of larger aggregates. The growth of colloidal nanoparticles follows a “two-stage” growth pattern, in which primary nanoparticles first nucleate in supersaturated solution and larger secondary particles aggregate.

As a result, as the amount of NaOH increases, the average particle diameter increases, and as the

amount of NaOH decreases, the average particle diameter decreases. In other words, it is observed that there is a direct proportional relationship between the amount of NaOH and the particle diameter.

Another situation that emerged during the experiment is the effects of the transfer rate on the size distribution. Accordingly, the faster Stock A is transferred, the narrower the distribution. In Figure 11, the length distribution that emerges in the slow transfer made for the 3 mol/L synthesis is seen. As a result, depending on the slowness of the transfer rate, the size distribution spreads over a wide range and shows irregularity.

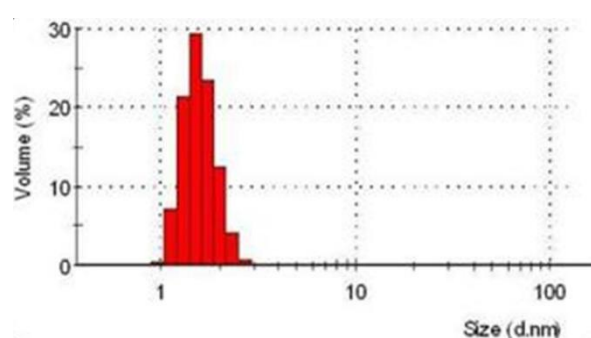


Fig. 9 DLS (2 mol/L) for B1 coded synthesis.

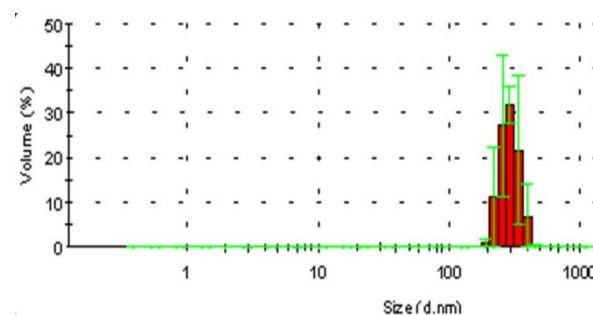


Fig. 10 DLS (3 mol/L) for B2 coded synthesis.

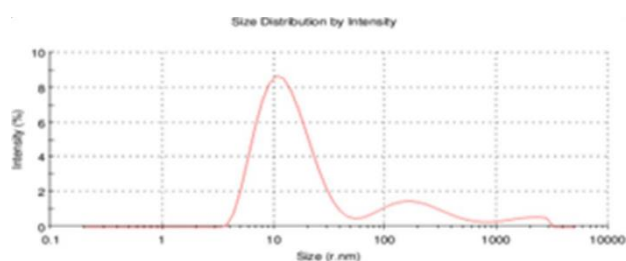


Fig. 11 Particle size distribution in the slow transfer process.

E. Effects of PAA amount on synthesis

The synthesis effect test of the amount of PAA was arranged according to the conditions in Table 3.

In the synthesis of 40 mmol, particles of about 10 nm are obtained, while in the synthesis of 0 mmol, particles of about 7nm, in the synthesis of 30 mmol, particles of about 100 nm, in the synthesis of 36 mmol large size distribution particles, in the synthesis of 50 mmol particles of about 6 nm were obtained in the synthesis (see Figure 12-15)

Table 3. Synthesis conditions determined for the effect of PAA amount.

Modification	Description	Code
Main Synthesis	40 mmol	A0
PAA Amount	0 mmol	D1
	30 mmol	D2
	36 mmol	D3
	50 mmol	D5

During the growth process, high concentrations of PAA effectively restrict the growth of the nanostructure. Compared to low concentrations, smaller sizes were reached at high concentrations.

The effects of the transfer rate on the size distribution were also seen in the 36 mmol synthesis. It is seen that the size distribution in the slow transmission in this synthesis is quite wide. If the transfer process was done faster, the expected effect would be to obtain particles larger than 10 nm.

As a result, as the amount of surfactant PAA (polyacrylic acid) increases, the average particle diameter decreases, and as the amount of PAA decreases, the average particle diameter increases; In other words, it was observed that there is an inversely proportional relationship between the amount of PAA and the particle diameter.

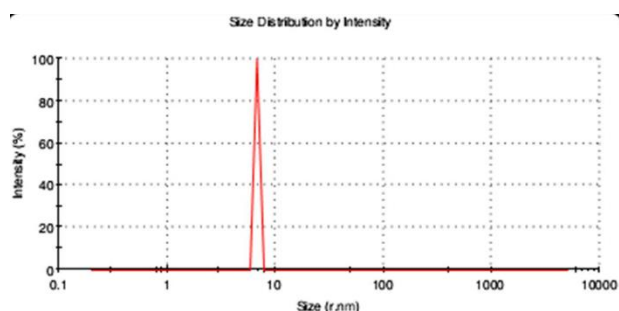


Fig. 12 DLS (0 mmol) for D1-coded synthesis.

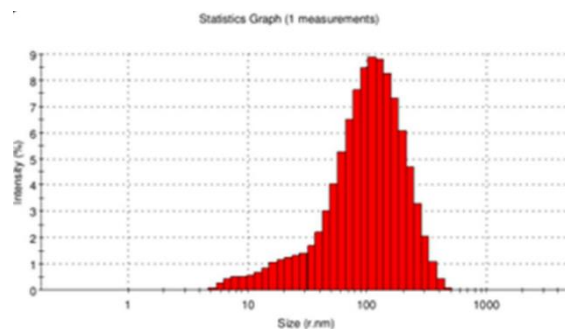


Fig. 13 DLS (30 mmol) for D2-coded synthesis.

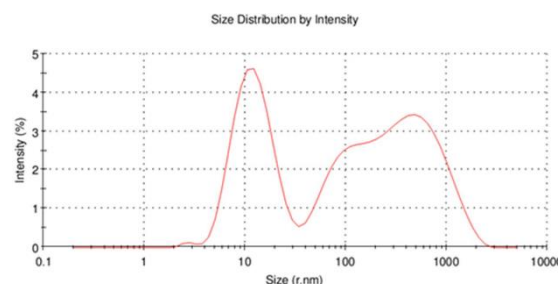


Fig. 14 DLS (36 mmol) for D3-coded synthesis.

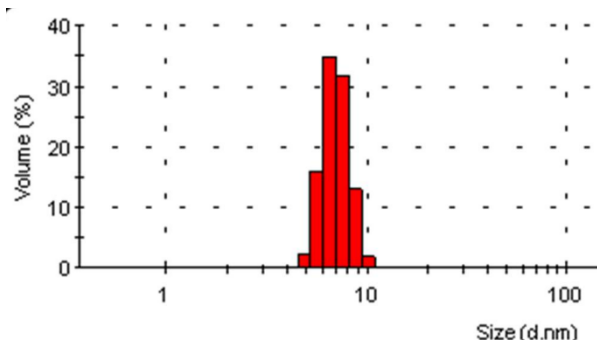


Fig. 15 DLS (50 mmol) for D5-coded synthesis.

Figure 16 shows the XRDs of the above-mentioned syntheses. Na and Cl peaks are also encountered due to the poor cleaning of NaCl from particles. The narrowness of the diffraction peaks in the productions with low PAA and the wideness in the multiples supports the inferences in the DLS measurements.

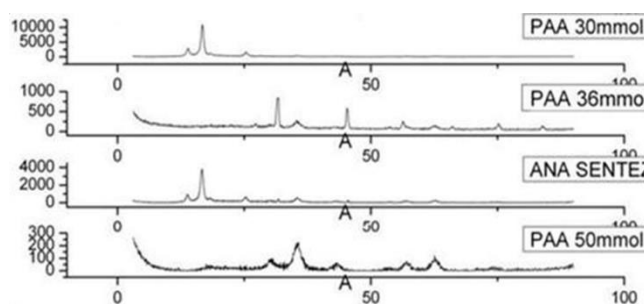


Fig. 16 XRDs for PAA experiments.

F. Effects of $FeCl_3$ amount on synthesis

The experiment of the effect of $FeCl_3$ amount on synthesis was arranged according to the conditions in Table 4. While particles of approximately 10 nm were obtained in the synthesis of 20 mmol, particles of approximately 40nm were obtained in the synthesis of 15 mmol, and particles of approximately 9 nm were obtained in the synthesis of 25 mmol (see Figure 17-19).

Table 4. Synthesis conditions determined for the effect of $FeCl_3$ amount.

Modification	Description	Code
Main Synthesis	20 mmol	A0
$FeCl_3$ Amount	15 mmol	E1
	25 mmol	E2

During the growth process, high concentrations of $FeCl_3$ effectively restrict the growth of the nanostructure. Compared to low concentrations, smaller sizes were reached at high concentrations.

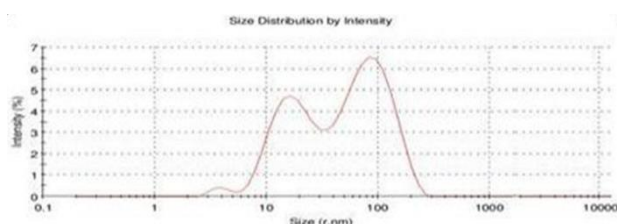


Fig. 17 DLS (15 mmol) for E1-coded synthesis.

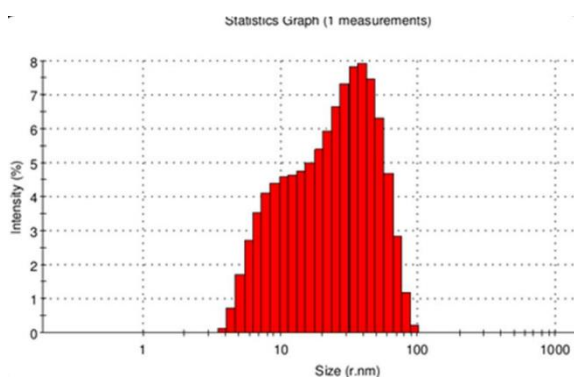


Fig. 18 DLS (15 mmol) for E1-coded synthesis.

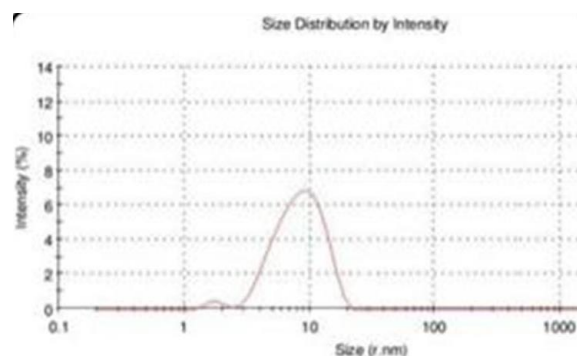


Fig. 19 DLS (25 mmol) for E2 coded synthesis.

The effects of the transfer rate on the size distribution were also seen in the 15 mmol synthesis. It is seen that the size distribution in the slow transmission in this synthesis is quite wide. A narrower particle distribution was achieved, as expected when the transfer process was performed faster.

As a result, as the amount of “precursor” $FeCl_3$ increases, the average particle diameter decreases, and as the amount of $FeCl_3$ decreases, the average particle diameter increases; In other words, it is observed that there is an inversely proportional relationship between the amount of $FeCl_3$ and the particle diameter.

G. Effects of reaction temperature on synthesis

The effect of reaction temperature on synthesis was arranged according to the conditions in Table 5. 190 °C was determined as the optimum temperature and no phase formation was observed as a result of transfers made at low temperatures such as 140 °C. According to this result, the transfer temperature also affects the formation of magnetite.

Table 5. Synthesis conditions determined for the effect of reaction temperature.

Modification	Description	Code
Main Synthesis	190 °C	A0
Reaction Temperature	140 °C	F1

IV. DISCUSSION

Maximum care should be taken in making all equipment used before synthesis clean, dry and moisture-free. A drying oven should be used to remove moisture from glass and metal items. Errors affecting stoichiometry should be avoided in weighing and transferring chemicals to the system (use of glove box is recommended). System

connections should be arranged according to the vacuum and gas passage characteristics (one-way valve before the bubble counter and a flow indicator can be added between the manifold and the system). Instead of removing the oxygen from the system by sweeping the nitrogen gas, with the "vacuum trap" immersed in liquid nitrogen, the oxygen can be liquefied before it enters, creating an environment free from moisture and oxygen.

By using thermal insulation (heater jacket) or high boiling point and stable liquids in oil bath, high temperatures can be reached in a shorter time, and the transfer process can be carried out faster and effortlessly by using expensive pressure compensating materials. If the particles are subjected to washing, drying and characterization processes as soon as possible after synthesis, they will be protected from external effects such as oxidation.

V. CONCLUSION

In this study, the synthesis of monodisperse magnetite colloidal aggregates by high temperature solution phase process is generally emphasized. It is seen from the studies that the size of the clusters can be regulated by changing the hydrolysis rate with the effect of NaOH. PAA chains attached to the surface form very soluble aggregates in water. Colloidal nanoparticles exhibit superparamagnetic behaviour at room temperature. The results for the synthesis can be summarized as follows.

As the amount of NaOH increases, the average particle diameter increases, as the amount of NaOH decreases, the average particle diameter decreases; In other words, it is observed that there is a direct proportional relationship between the amount of NaOH and the particle diameter.

As the amount of surfactant PAA (polyacrylic acid) increases, the average particle diameter decreases, as the amount of PAA decreases, the average particle diameter increases; In other words, it was observed that there is an inversely proportional relationship between the amount of PAA and the particle diameter.

As the amount of precursor FeCl_3 increases, the mean particle diameter decreases, as the amount of FeCl_3 decreases, the mean particle diameter increases; In other words, it is observed that there is an inversely proportional relationship between the amount of FeCl_3 and the particle diameter.

Transfer temperatures also affect the magnetite formation. $190\text{ }^\circ\text{C}$ was determined as the optimum temperature and no phase formation was observed as a result of transfers made at low temperatures such as $140\text{ }^\circ\text{C}$.

The effects of the transfer rate on the size distribution were observed. It is seen that the size distribution in the slow transmission is quite wide. A narrower particle distribution was achieved, as expected when the transfer process was performed faster.

Magnetic fluids prepared according to the observations can remain stable for a long time. Even after weeks, $\text{Fe}_3\text{O}_4@\text{PAA}$ particles are still well dispersed in the liquid and no precipitation is observed. Based on these results, the reaction conditions that need to be controlled for the synthesis of magnetic liquids with the desired properties is outlined in general terms.

REFERENCES

- [1] U. Nisar, N. Muralidharan, R. Essehli, R. Amin, and I. Belharouak, "Valuation of Surface Coatings in High-Energy Density Lithium-ion Battery Cathode Materials," *Energy Storage Mater.*, vol. 38, pp. 309–328, Jun. 2021, doi: 10.1016/j.ensm.2021.03.015.
- [2] K. S. C. M, S. H, Sangeeta, and M. CB, "A Review: The Uses of Various Nanoparticles in Organic Synthesis," *J. Nanomed. Nanotechnol.*, vol. 11, no. 2, 2020, doi: 10.35248/2157-7439.19.10.543.
- [3] R. P. Das and A. K. Pradhan, "An Introduction to Different Methods of Nanoparticles Synthesis," in *Bio-Nano Interface*, Singapore: Springer Singapore, 2022, pp. 21–34.
- [4] H. Jan *et al.*, "A detailed review on biosynthesis of platinum nanoparticles (PtNPs), their potential antimicrobial and biomedical applications," *J. Saudi Chem. Soc.*, vol. 25, no. 8, p. 101297, Aug. 2021, doi: 10.1016/j.jscs.2021.101297.
- [5] S. C. Carroccio, P. Scarfato, E. Bruno, P. Aprea, N. T. Dintcheva, and G. Filippone, "Impact of nanoparticles on the environmental sustainability of polymer nanocomposites based on bioplastics or recycled plastics – A review of life-cycle assessment studies," *J. Clean. Prod.*, vol. 335, p. 130322, Feb. 2022, doi: 10.1016/j.jclepro.2021.130322.
- [6] N. Basavegowda and K.-H. Baek, "Multimetallic Nanoparticles as Alternative Antimicrobial Agents: Challenges and Perspectives," *Molecules*, vol. 26, no. 4, p. 912, Feb. 2021, doi: 10.3390/molecules26040912.
- [7] A. G. Díez, M. Rincón-Iglesias, S. Lanceros-Méndez, J. Reguera, and E. Lizundia, "Multicomponent magnetic nanoparticle engineering: the role of structure-property relationship in advanced applications," *Mater. Today Chem.*, vol. 26, p. 101220, Dec. 2022, doi: 10.1016/j.mtchem.2022.101220.

- [8] T. Ming, B. Dietzek-Ivanšić, X. Lu, X. Zuo, and V. Sivakov, "Silicon Nanowires Decorated with Silver Nanoparticles for Photoassisted Hydrogen Generation," *ACS Appl. Energy Mater.*, vol. 5, no. 6, pp. 7466–7472, Jun. 2022, doi: 10.1021/acsaem.2c00968.
- [9] G. Wang *et al.*, "Colloidal Nanocrystals Fluoresced by Surface Coordination Complexes," *Sci. Rep.*, vol. 4, no. 1, p. 5480, Jun. 2014, doi: 10.1038/srep05480.
- [10] J. Medinger, M. Nedyalkova, and M. Lattuada, "Solvothermal Synthesis Combined with Design of Experiments—Optimization Approach for Magnetite Nanocrystal Clusters," *Nanomaterials*, vol. 11, no. 2, p. 360, Feb. 2021, doi: 10.3390/nano11020360.
- [11] E. M. Materón *et al.*, "Magnetic nanoparticles in biomedical applications: A review," *Appl. Surf. Sci. Adv.*, vol. 6, p. 100163, Dec. 2021, doi: 10.1016/j.apsadv.2021.100163.
- [12] K. Q. Jabbar, A. A. Barzinjy, and S. M. Hamad, "Iron oxide nanoparticles: Preparation methods, functions, adsorption and coagulation/flocculation in wastewater treatment," *Environ. Nanotechnology, Monit. Manag.*, vol. 17, p. 100661, May 2022, doi: 10.1016/j.enmm.2022.100661.
- [13] K. J. Mohammed, S. K. Hadrawi, and E. Kianfar, "Synthesis and Modification of Nanoparticles with Ionic Liquids: a Review," *Bionanoscience*, vol. 13, no. 2, pp. 760–783, Jun. 2023, doi: 10.1007/s12668-023-01075-4.
- [14] D. Wen *et al.*, "Size and Composition Control of Magnetic Nanoparticles," *J. Phys. Chem. C*, vol. 127, no. 19, pp. 9164–9172, May 2023, doi: 10.1021/acs.jpcc.3c01275.
- [15] M. D. Nguyen, H.-V. Tran, S. Xu, and T. R. Lee, "Fe₃O₄ Nanoparticles: Structures, Synthesis, Magnetic Properties, Surface Functionalization, and Emerging Applications," *Appl. Sci.*, vol. 11, no. 23, p. 11301, Nov. 2021, doi: 10.3390/app112311301.
- [16] S. Mourdikoudis *et al.*, "Oleic acid/oleylamine ligand pair: a versatile combination in the synthesis of colloidal nanoparticles," *Nanoscale Horizons*, vol. 7, no. 9, pp. 941–1015, 2022, doi: 10.1039/D2NH00111J.
- [17] V. Ganesan, B. B. Lahiri, C. Louis, J. Philip, and S. P. Damodaran, "Size-controlled synthesis of superparamagnetic magnetite nanoclusters for heat generation in an alternating magnetic field," *J. Mol. Liq.*, vol. 281, pp. 315–323, May 2019, doi: 10.1016/j.molliq.2019.02.095.
- [18] M. Kole and S. Khandekar, "Engineering applications of ferrofluids: A review," *J. Magn. Magn. Mater.*, vol. 537, p. 168222, Nov. 2021, doi: 10.1016/j.jmmm.2021.168222.
- [19] S. Küçükdermenci, "Synthesis of magnetic field responsive colloidal nanoparticles and structural, magnetic, magneto-optic and magneto-caloric characterization," Ege University, 2012.
- [20] S. Küçükdermenci, D. Kutluay, and İ. Avgın, "Synthesis of a Fe₃O₄/PAA-based magnetic fluid for Faraday-rotation measurements," *Mater. Tehnol.*, vol. 47, no. 1, pp. 71–78, 2013.
- [21] S. Küçükdermenci, D. Kutluay, E. Çelik, Ö. Mermer, and A. İbrahim, "Concentration and path-length dependence on the Faraday rotation of magnetic fluids based on highly water-soluble Fe₃O₄/PAA nanoparticles synthesized by a high-temperature hydrolysis method," *Mater. Tehnol.*, vol. 47, no. 3, pp. 323–328, 2013.